ADVANCED MATERIALS TECHNOLOGIES
www.advmattechnol.de



# Food-Materials-Based Edible Supercapacitors

*Xu Wang, Wenwen Xu, Prithwish Chatterjee, Cheng Lv, John Popovich, Zeming Song, Lenore Dai, M. Yashar S. Kalani, Shelley E. Haydel, and Hanqing Jiang**

Novel and innovative medical technologies and devices have emerged to treat various diseases, such as deep brain stimulators for Parkinson's diseases,[1] vagal nerve stimulators for epilepsy,[2] electronic aspirin for head or facial pains,[3] and insulin pumps for diabetes,[4,5] among others. Although implantable electronic devices have revolutionized the care of patients, they harbor shortcomings such as the need for operations and perioperative complications. Biodegradable electronics and recent bioresorbable devices, such as individual transistors,[6] primary battery and biosensors,[7–11] organic field effect transistors,[12–14] organic transistors fabricated on bioresorbable substrates,[15] and many other advances,[16–18] provide alternative options to implantable electronics. Although biodegradable electronics resolve the issue of repeat surgery, they have other inherent shortcomings, for example low energy density and size limitation in biodegradable batteries.[9] In addition to implantation of permanent and biodegradable devices, the digestive system may serve as another route for administration of electronics that can modulate cellular and organ function without the need for implantation. Although some groups have proposed edible materials in the past, these materials still contain toxic components such as MnO2 which can cause abdominal pain and nausea by ingestion according to the National Institutes of Health (NIH).[19–22] Human dependence on food and digestion for over 200 000 years of evolution has allowed us to optimize timing and passage of materials through the alimentary tract. Here, this Communication uses the accumulated knowledge in the food industry, material sciences, device fabrication, and biomedical engineering and demonstrates fully functional and edible supercapacitors with the potential to work in the alimentary tract. Instead of using traditional noninert metals (e.g., iron, magnesium, and zinc), dielectric, and semiconducting materials (e.g., silicon) that can only be taken in very tiny amount at the level of micrograms per day, we adopted electrically conductive and chemically stable carbon (in the form of activated charcoal) and inert metals (edible gold), as well as other food sources in the fabrication of edible supercapacitors. In this Communication, we studied some edible materials and their performance as components for a supercapacitor. Most importantly, for the first time, we demonstrated that a single edible supercapacitor in the size of a standard capsule possesses enough energy and power to function as a standalone device to exhibit antibacterial activity by killing disease-causing bacteria *in vitro*. Also, we demonstrate that, as energy storage device, these supercapacitors connected in series are sufficiently powerful to drive a commercial camera.

**Figure 1**a shows a schematic illustration of a representative supercapacitor in the explosive view, which contains package, current collectors, electrode materials, electrolyte, and separator. All components are either food supplement, additive or explicit food, which are also detailed in Figure 1a as an example. A photograph of an opened supercapacitor is shown in Figure 1b, with the activated charcoal as the electrode, cheese as the segregation layer, and seaweed as the separator. Taking the components shown in Figure 1a,b as an example, here activated charcoal (Nature's Way Products, Inc.; Green Bay, WI) from dietary supplement capsules was used as electrode materials. Figure 1c shows the transmission electron microscopy (TEM) image of activated charcoal, revealing that the size of an individual carbon particle is around 100 nm. As seen in Figure 1d, the surface area of the activated charcoal is ≈1400 $m^2 g^{-1}$, which is comparable to activated carbon materials used in the majority of supercapacitors.[23] In order to bind discrete active charcoal particles into a continuum film as electrodes, edible binders are employed. Egg whites, widely used binding additive in food processing, were used as binders in electrodes. The presence of hydrogen bonds and ionic interactions with proteins allows the formation of films with high adhesive strength,[24–26] which allows egg whites to be used as binders in food processing industries. The inert metals, such as very thin gold leaves that appear in artisan baking and many Eastern cuisines, are used as current collectors. Gold leaves are safe to intake with purity higher than 23 karat and in fact gold is called E175 in food production nomenclature within the European Union. The sheet resistance of the gold leaf with a thickness of 3–5 μm was measured to be 0.48 Ω $sq^{-1}$ by four-point probe.

The superior properties of activated charcoal and gold leaves, namely, high electrical conductivity and chemical stability,

X. Wang, W. Xu, Dr. P. Chatterjee, C. Lv, Z. Song, Prof. L. Dai, Prof. H. Jiang
School for Engineering of Matter Transport and Energy
Arizona State University
Tempe, AZ 85287, USA
E-mail: hanqing.jiang@asu.edu
J. Popovich, Prof. S. E. Haydel
School of Life Sciences
Arizona State University
Tempe, AZ 85287, USA
Dr. M. Y. S. Kalani
Division of Neurological Surgery
Barrow Neurological Institute
St. Joseph's Hospital and Medical Center
Phoenix, AZ 85003, USA
Prof. S. E. Haydel
Center for Infectious Diseases and Vaccinology
The Biodesign Institute
Arizona State University
Tempe, AZ 85287, USA

DOI: 10.1002/admt.201600059

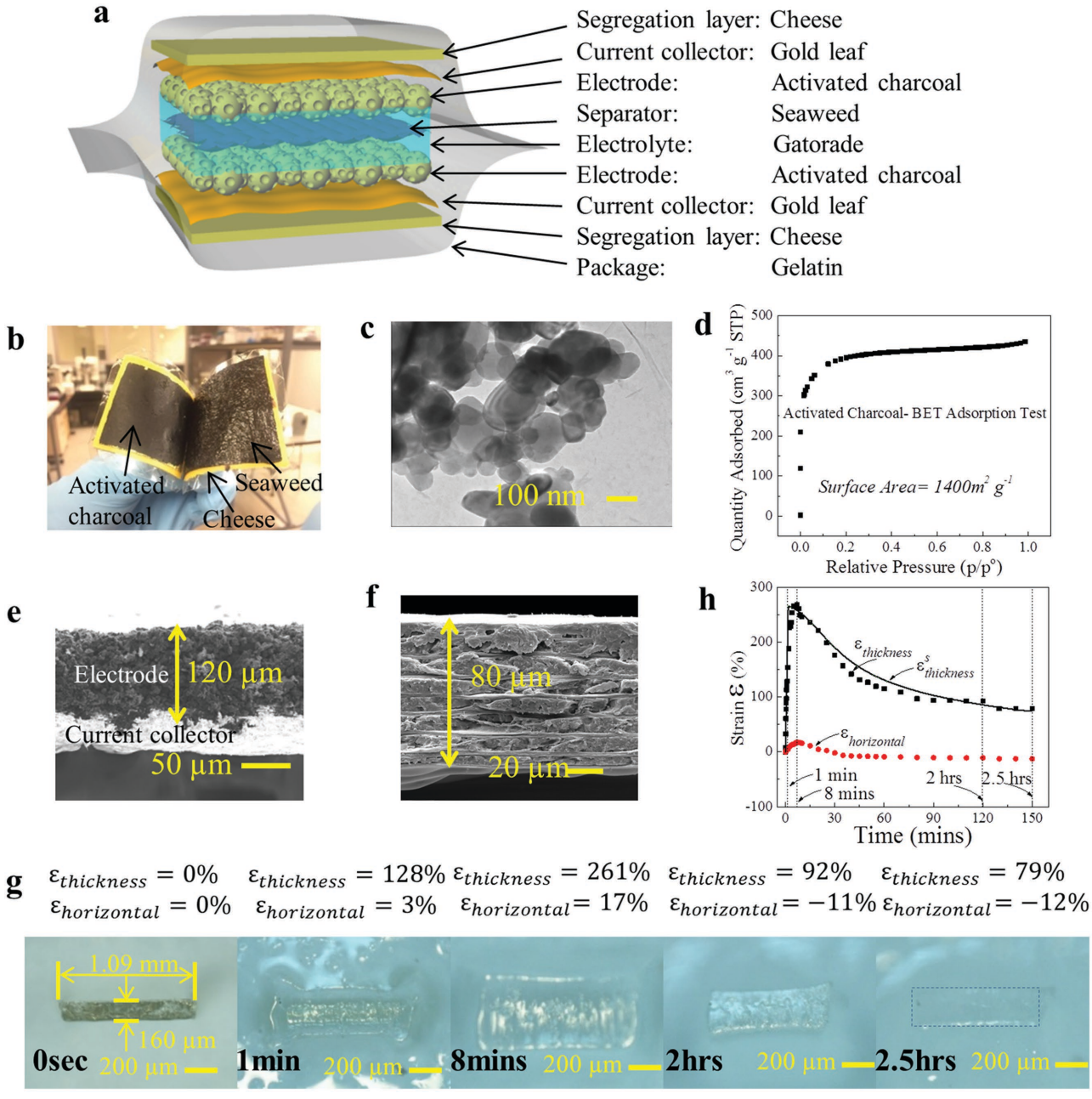


**Figure 1.** Illustration and materials analysis of the edible supercapacitor. a) Schematic structural illustration of an edible supercapacitor. b) An opened supercapacitor showing the activated charcoal electrode, seaweed separator, cheese segregation layer and gelatin package. c) TEM image showing that the particle size of activated charcoal is about 100 nm. d) Brunauer–Emmett–Teller (BET) test demonstrating the surface area of the activated charcoal is ≈1400 $m^2$ $g^{-1}$. e) SEM image of the cross-section of activated charcoal electrode. f) Cross-section photograph of seaweed separator showing the multilayer structure. g) Dissolution test of the gelatin in simulated gastric fluid. The gelatin becomes indistinguishable from water after 2.5 h. h) The time evolutions of the strains obtained from experiments and simulations. $\varepsilon_{thickness}$ is the strain in thickness direction from experiment, $\varepsilon^{s}_{thickness}$ is the strain in thickness direction from simulation, and $\varepsilon_{horizontal}$ is the strain in horizontal direction from experiment. The horizontal strain is neglected in the simulation as it is much smaller than that in the thickness direction. Thus the simulation is a 1D case.

empower them great applications in edible electronics. Particularly their high chemical stabilities allow one to intake large amount. For example, activated charcoal can be administered 100 g in a single dose,[27,28] though this high dose may cause pulmonary aspiration.[29] However, it will be noticed that one does not need to reach this extreme case as this Communication will show that less than 1 g of active charcoal is sufficient to store enough energy to power a commercial device. No specific dosage restriction is imposed on edible gold leaves as food additive. On the contrary, other metals usually used in biodegradable and bioresorbable electronics (such as iron, magnesium, and zinc) can only be taken no more than 0.03, 0.4, and 0.015 g

correspondingly on a daily basis according to the NIH, which greatly limits their applications.

Figure 1e shows the scanning electron microscopy (SEM) image of the electrode cross-section with a typical thickness of 120 μm. The separator needs to be permeable to ions and display high electrical resistance to avoid the electrical contact between the electrodes. Here, we demonstrate roasted seaweed, a popular snack and also heavily used in sushi, with multilayer hydrophilic structures as one of the possible separators. Figure 1f shows the SEM image of the roasted seaweed in a cross-sectional view, where the multilayer structure is seen. The permittivity of the roasted seaweed was measured to be 52 $g^{-1}$ $m^2$ $s^{-1}$.

Other components such as package and electrolyte have also been studied. Gelatin sheets (Modernist Pantry, LLC; York, ME), used in food processes and many medical capsules, were employed as the package materials. Figure 1g shows a cross-sectional view of an *in situ* observation of a digestion process in room temperature at 25 °C when a gelatin sheet was immersed in the simulated gastric fluid and constrained in the horizontal direction (Figure S1, Supporting Information). It is observed that a gelatin sheet with an initial cross-sectional area of 160 μm × 1090 μm first swells due to the diffusion of the gastric fluid into the polymeric gelatin network and then shrinks due to the digestion of gelatin and eventually becomes indistinguishable from simulated gastric fluid microscopically (Nikon eclipse lv100, 5X objective) after 2.5 h, which is assumed to be dissolved since it no longer maintains enough mechanical strength to serve as a package. During this process (swelling → shrinking), because of the constraint in the horizontal direction, the maximum strain in the horizontal direction $\varepsilon_{horizontal}$ is only 17%, while its counterpart in the thickness direction $\varepsilon_{thickness}$ is 261%. This quasi-1D constrained digestion process can be understood by a theoretical model that considers the coupling of mass diffusion, chemical reaction, and extremely large mechanical deformation. As shown in Figure 1h, the time evolutions of the strains ($\varepsilon_{horizontal}$ and $\varepsilon_{thickness}$) obtained from experiments and simulations agree very well. Many previous studies by other groups have shown that by crosslinking treatment, gelatin is able to last much longer in humid, acidic, and elevated temperature environment.[30–32] Our ongoing work of gelatin treatment based on surface modification and crosslinking is expected to make gelatin dissolution controllable.

A polyelectrolyte drink such as Gatorade (Chicago, IL) with high concentrations of sodium, potassium, citrate, and other stabilizing agents and high ionic conductivity (>2 mS $cm^{-1}$) was used as the electrolyte. Cheese slices (Lucerne Foods, Inc.; Pleasanton, CA) were placed between the highly hydrophilic gelatin sheet (package) and gold leaf (current collector) as a segregation layer to avoid direct contact of gelatin and electrolyte. Finally, the package was sealed thermally by an impulse sealer with controlled heat. Thus, an entirely edible supercapacitor was assembled by all edible materials, including activated charcoal, egg white, gold leaf, roasted seaweed, Gatorade, cheese, and gelatin.

**Figure 2**a presents the cyclic voltammetry (CV) curves of the edible supercapacitor at the scanning rates from 5 to 100 mV $s^{-1}$. The CV curves are of clearly rectangular shape at lower scanning rates and become approximately rectangular shape at increased scanning rates, which are ideal for capacitive properties and reversibility of a supercapacitor. The galvanostatic charge/discharge testing result (Figure 2b) shows some internal resistance with a constant current density of 1 A $g^{-1}$. After 1000 charge/discharge cycles (Figure 2c), the specific capacitance retains 92.3% by dropping from 78.8 to 72.7 F $g^{-1}$ under 1 A $g^{-1}$ current density, which is consistent with activated carbon-based supercapacitors.[33] The degradation mainly results from the electrolyte absorption by the gelatin sheet. To confirm, aluminized polyethylene (PE) (standard packing materials for supercapacitors) and gelatin without cheese segregation have been tested for comparison. The specific capacitance using aluminized PE retains 96.9% by dropping from 76.4 to 74.0 F $g^{-1}$ after 1000 charge/discharge cycles and thus demonstrates excellent electrochemical stability of the electrode–separator–electrolyte system. However, the specific capacitance with gelatin drops more than 50% from 73.2 F $g^{-1}$ to less than 34.9 F $g^{-1}$ in 100 cycles and to 4.4 F $g^{-1}$ in 1000 cycles. This comparison shows that cheese slices can significantly prevent electrolyte loss and improve the cycling stability. Figure 2d presents the electrochemical impedance spectroscopy (EIS) results after one cycle and 1000 cycles using gelatin sheet with cheese as the packing materials. Only slight resistance increase was observed. Figure 2e shows the energy and power densities curve calculated from the constant current density charge–discharge curves measured with 250 mA $g^{-1}$, 500 mA $g^{-1}$, 1 A $g^{-1}$, 2 A $g^{-1}$, and 4 A $g^{-1}$ current densities. The leakage current was measured to be 0.08 mA, which is at the same level of typical supercapacitors. The leakage current profile is shown in Figure S2 (Supporting Information).

The material possibilities of edible supercapacitors are immense due to the vast number of available food products. Table S1 (Supporting Information) provides a list of many other materials investigated including monosodium glutamate (MSG, a flavor enhancer) as electrolyte additive to increase the electrolyte ions density, carboxymethyl cellulose (a food additive) as binder, silver leaf as current collector, V8 vegetable drink and Monster Energy drink as liquid electrolytes, BBQ sauce, jello, and cheese as gel electrolytes, and gummy candy as package material. In Figure 2f, for 1000 charge–discharge cycles at the current density of 1 A $g^{-1}$, the specific capacitance increases from 78.8 to 129 F $g^{-1}$ after the addition of MSG in Gatorade due to the increase of ion densities. The specific capacitances of other liquid electrolytes (V8 vegetable and Monster Energy drinks) show different values due to different ions components and concentrations. Due to high internal resistance, the specific capacitances with gel electrolytes (BBQ sauce, jello, and cheese) are lower than those with liquid electrolytes (Figure S3, Supporting Information). In the following electrochemical characterization, we use activated charcoal, gold leaf, Gatorade, seaweed, egg white, cheese, and gelatin as the model materials for edible supercapacitors.

Figure 2g demonstrates a supercapacitor set lighting up a light-emitting diode (LED) inside the simulated gastric fluid. The supercapacitor set consists of three supercapacitors (electrode area is 2 cm × 2 cm) connected in series. The LED stayed on for 3 min, followed by gradual dimming and lack of emission after 4 min. After 1 h, the supercapacitor was partially dissolved in the simulated gastric fluid. Figure S4 (Supporting Information) shows the supercapacitor set turning

ADVANCED MATERIALS TECHNOLOGIES
www.advmattechnol.de

Materials Views
www.MaterialsViews.com

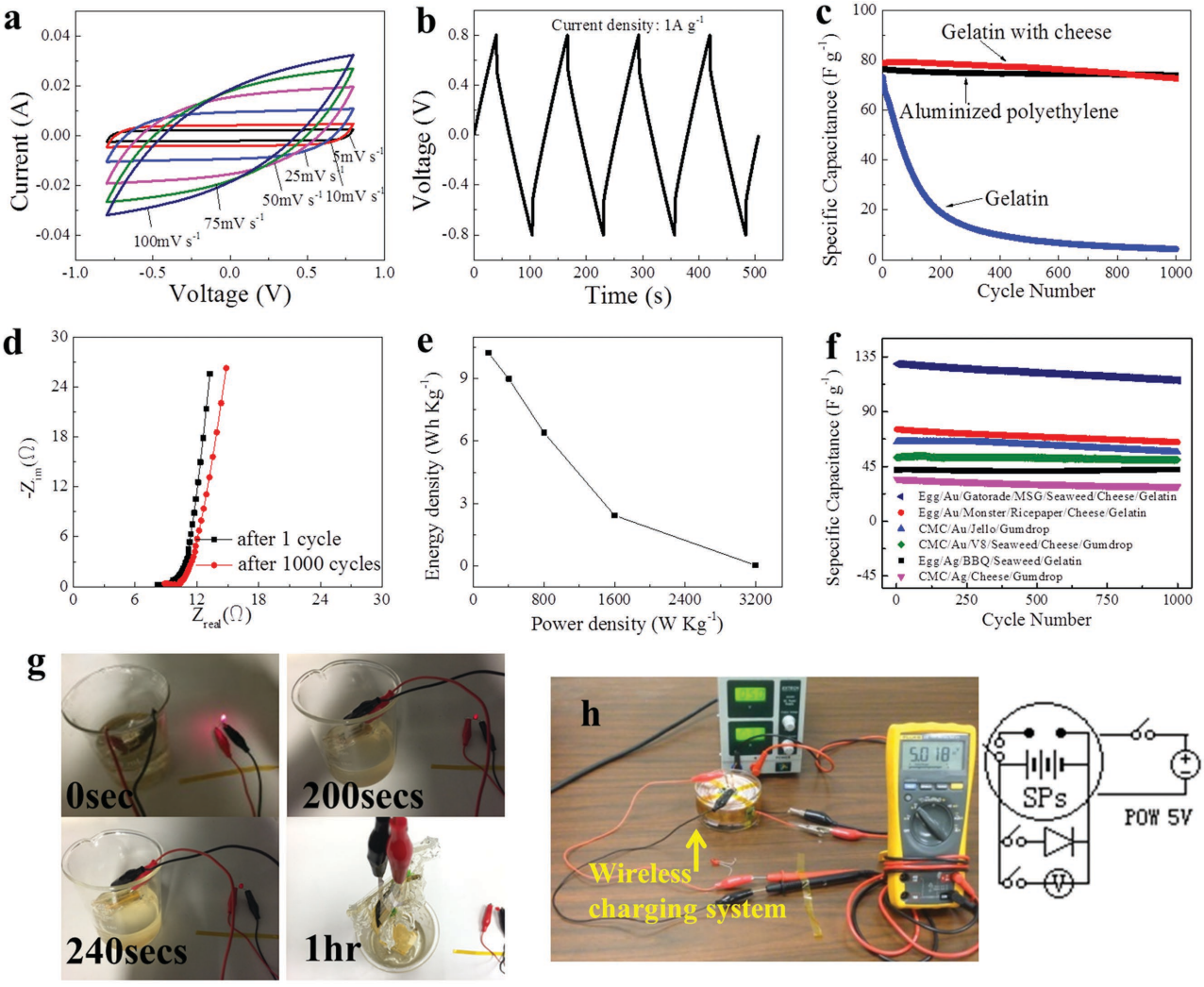


**Figure 2.** Electrochemical characterizations of edible supercapacitors and demonstration of edible supercapacitors powering an LED in simulated gastric fluid. a) CV curves at the scanning rates from 5 to 100 mV $s^{-1}$. b) Galvanostatic charge–discharge voltage profiles of edible supercapacitor with a constant current of 1 A $g^{-1}$. c) Galvanostatic charge–discharge cycles measured with a constant current of 1 A $g^{-1}$, for supercapacitor with gelatin and cheese slides, with aluminized polyethylene (PE), and with gelatin only as package materials. d) Electrochemical impedance spectroscopy (EIS) analysis before the first discharge cycle and after 1000 charge–discharge cycles. e) Energy and power densities calculated from the constant current density charge–discharge curves measured with 250 mA $g^{-1}$, 500 mA $g^{-1}$, 1 A $g^{-1}$, 2 A $g^{-1}$, and 4 A $g^{-1}$. f) 1000 charge–discharge cycling at a constant current density of 1 A $g^{-1}$ for supercapacitors with different materials combinations. g) Images of supercapacitor set lighting up an LED in simulated gastric solution. h) The supercapacitor integrated with a receiver coil and AC–DC converting circuit placed in a charging chamber can be wirelessly charged, which is illustrated in an image and a circuit layout.

on the LED outside of the fluid. Supercapacitor has the intrinsic shortcoming of low energy density. When supercapacitor is in human body, wire charging would be almost impossible. To extend the working time of supercapacitors, a novel wireless charging system was developed (Figure 2h). The supercapacitor integrated with a receiver coil and AC–DC converting circuit (GHH) placed in a charging chamber can be charged wirelessly in the alternating electromagnetic field (with a frequency of 60 Hz) created by the transmitter coil and DC–AC converting circuit (GHH) outside the charging chamber (Figures S5–S7 and Movie S1, Supporting Information). This novel strategy simulates a scenario where a supercapacitor is inside a human body while it can be wirelessly charged in an alternating electromagnetic field that surrounds the human body.

The antibacterial activity of electric current has previously been demonstrated against planktonic *Escherichia coli*, *Klebsiella pneumoniae*, and *Proteus* species in various liquids including synthetic urine, water, and salt solutions.[34–38] Moreover, low-intensity electric current reduced the numbers of viable bacteria in staphylococcal and *Pseudomonas* biofilms after prolonged exposure (1–7 d).[39,40] However, thus far, no real device that can be taken into human body and used to kill bacteria via low-intensity electric current has been demonstrated. Here, to further assess potential biomedical applications of the edible supercapacitor, the effect of edible supercapacitor-discharged electric current on bacterial viability was investigated using *E. coli* ATCC 25922 in broth antimicrobial susceptibility experiments. **Figure 3**a presents the edible supercapacitor packaged

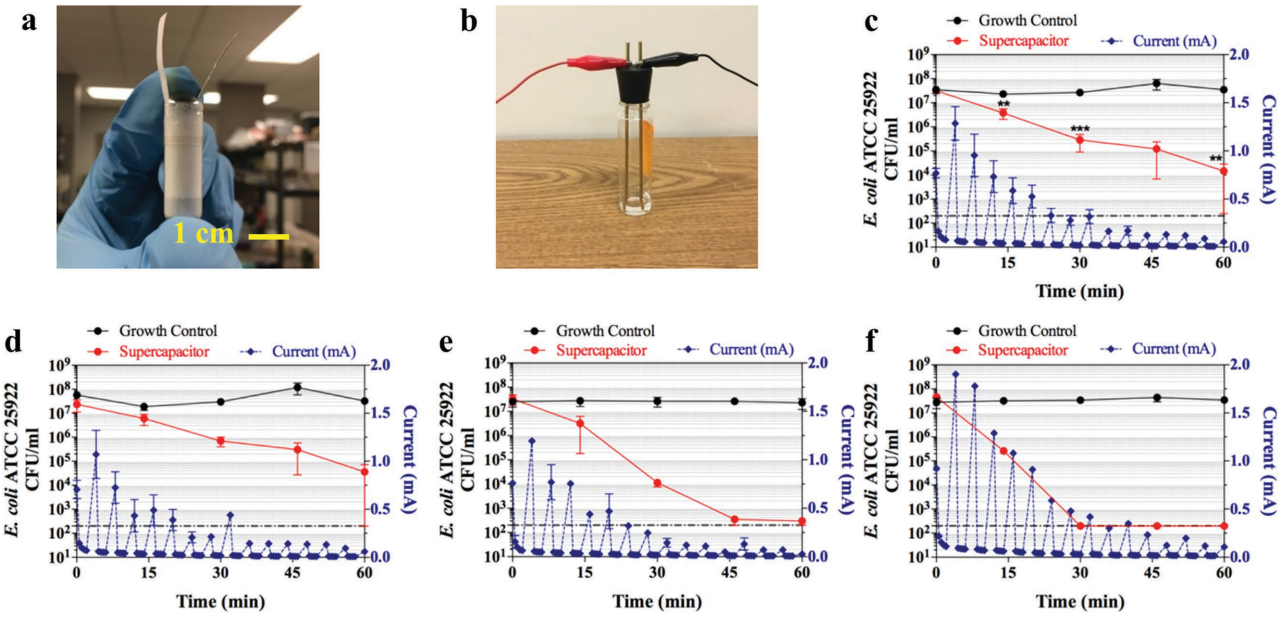


**Figure 3.** *E. coli* survival upon exposure to supercapacitor-mediated electric current. a) Image of an edible supercapacitor packaged in a standard 000 size capsule. b) Image of two brass rods stabilized with a rubber stopper and inserted into the 3 mL *E. coli*-PBS suspension. c) Exponential-phase *E. coli* was exposed to alternating on–off supercapacitor-mediated electric current for 60 min. Values represent the mean colony-forming units (CFU) and standard error of the mean (SEM) of five independent experiments. Average current (mA) measurements and SEM of the five independent experiments are shown on the right *y*-axis. Correlation ($r = 0.9934$) between electric current and bacterial viability for the five independent experiments was determined using Pearson unpaired correlation coefficient. $^{**}P < 0.01$; $^{***}P < 0.001$; unpaired *t*-test with Holm-Sidak multiple comparisons. Results of d,e) replicate experiments or f) a single experiment with varying supercapacitor currents demonstrate that increasing low-intensity amperage correlates with greater reductions in bacterial viability ($r = 0.9673$, $r = 0.9969$, and $r = 0.9960$, respectively). The detection limit (hatched line) for all experiments was 200 CFU $mL^{-1}$.

in standard 000 size gelatin capsule. Figure 3b shows two brass rods with stopper inserted into a 3 mL *E. coli*-PBS suspension. The electric current loop was formed by connecting the outside ends of the rods with the supercapacitor. Exponential-phase *E. coli* cells (≈$10^7$ CFU $mL^{-1}$) were resuspended in phosphate-buffered saline (PBS) and exposed to alternating on (2 min) and off (2 min) cycles of electric current for 60 min. Compared to no electric current (growth control), we detected a significant reduction ($P < 0.01$) in the number of viable cells present after exposure to supercapacitor-mediated electric current for 60 min (Figure 3c). A time-dependent reduction in bacterial viability was observed, with generally lower viable cell counts detected when electric current was applied for longer periods of time. The edible supercapacitor causes significant bactericidal activity reduction (99.93% average reduction) after 60 min of alternating on–off current exposures (Figure 3c). When the replicate experiments were separated based on amperage readings, a higher amperage correlated with a greater reduction in bacterial viability at all time points (Figure 3c–f), suggesting that proper design of edible supercapacitors better controls the efficiency of antibacterial activity. This shows that a single supercapacitor in standard capsule possessed enough energy and power for potential practical medical applications.

Another promising application of edible supercapacitors is to function as the electrical source for powering an endoscope. Here we demonstrated that the edible supercapacitors are able to power a USB endoscope inspection snake tube camera (Silicon Electronic). A USB cable connected to a computer is originally designed for powering the camera and enabling data transmission. To demonstrate our supercapacitors, the positive and negative (ground) power cables of the USB snake camera were cut off and only the data cables were connected to a computer for data transmission (**Figure 4**a). Five fully charged 4 cm × 4 cm (electrode area) square supercapacitors with an average mass loading of 0.08 g were connected in series to output a 5 V voltage for powering the USB camera that requires minimum 3.3 V working voltage. The negative terminal of the supercapacitors was connected to the negative (ground) of the snake camera at the beginning to maintain the same reference potential between the computer and supercapacitor. After the positive terminal of the supercapacitors was connected with the positive cable of the snake camera, the camera was recognized and output a 320 × 240 pixels video on the computer screen (Figure 4b). The current was measured to be 35 mA. By sweeping the camera back and forth and pointing at the computer screen, the image was captured and shown on the computer screen. The power cables were then disconnected from the supercapacitors, and one of the supercapacitors was removed and cut open (Figure 4c). The cross-section of the opened supercapacitor is shown in Figure 4d. Finally, the removed supercapacitor was eaten (Figure 4e) and swallowed (Figure 4f). Supporting Information Movie S2 shows this demonstration.

The edible supercapacitor presented in this Communication is the first one that is truly edible and digestible as all components are either food supplement, additive, or explicit food,

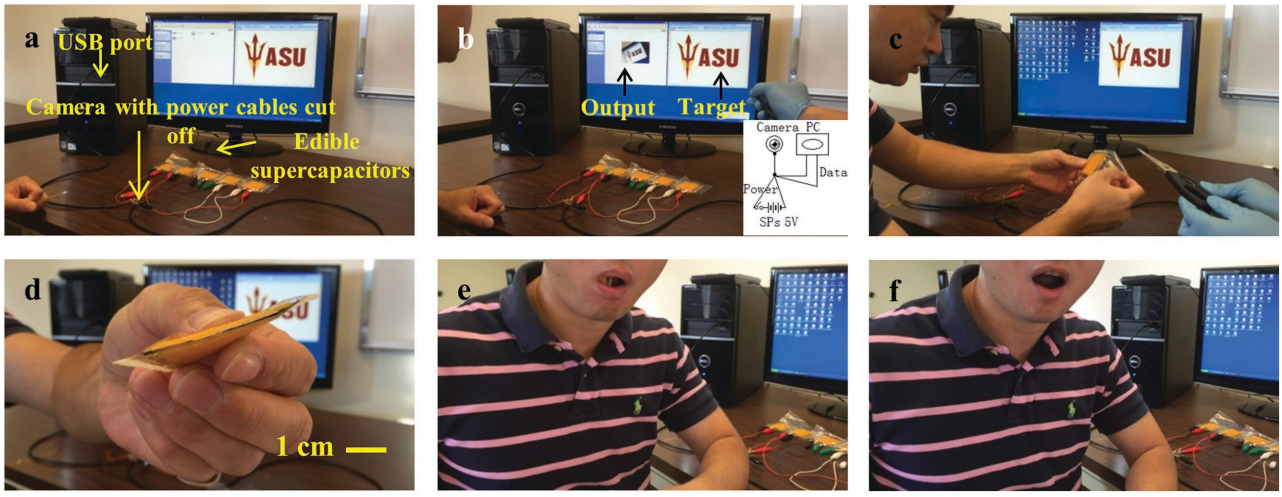


**Figure 4.** Edible supercapacitors powering a snake camera and being eaten. a) A snake camera with power cables disconnected was plugged in a USB port. Five fully charged supercapacitors were connected in series to output a 5 V voltage. b) After the supercapacitor was connected to the USB power cables, the snake camera was recognized and output a video. The inset is the circuit layout showing the connection. c,d) A corner of one supercapacitor was cut out. e,f) The removed corner was chewed and swallowed.

which is different from other endeavors on edible electronics or edible energy storage devices. As a standalone device, the edible supercapacitors have demonstrated their ability to serve as an electrical "antibacterial" for killing bacteria (e.g., *E. coli*) *in vitro* which renders huge potential for curing bacteria-caused diseases in alimentary system from mouth to intestine. The supercapacitors have also demonstrated to power a commercial USB camera which indicates a promising energy source for biomedical devices. It has not escaped our attention that this edible electronic device, in addition to its antibacterial properties, may be used as an oncological adjuvant for alimentary and other malignancies. In order to develop fully edible and digestible electronics, integration of edible energy source and other edible functional devices (e.g., circuits) is indispensable and necessitates further research studies.

## Experimental Section

*Fabrication of Edible Supercapacitors and Electrochemical Measurements*: The slurry was prepared by mixing the activated charcoal (Nature's Way Products, Inc.; Green Bay, WI) with egg white (mass ratio of 1:2). Egg whites primarily contain biotin and proteins such as albumin, mucoproteins, and globulins that are able to form a biomacromolecule solution with water through hydrogen bonding between the proteins and water. Deionized water was then added into the mixture (activated charcoal to water ratio of 1:3). The mixture was magnetic stirred for 2 h followed by an ultrasonication for 30 min in water bath. The current collector was prepared by applying egg white uniformly on chlorine-free wood fiber paper (Mondi; Graz-Seiersberg, Austria) to form an adhesive layer, then attaching ≈3 µm thick 23 kt edible gold leaf (Alma Gourmet Ltd; Long Island City, NY) on the paper. The gold-coated paper was then dried in ambient environment for 2 h before being patterned into the current collector with desired areas. The slurry was coated on the current collector by doctor's blading followed by overnight drying in ambient environment and 6 h drying in room temperature, low pressure (10 Pa) chamber to avoid thermal stress as well as remove the water in the electrode. A typical thickness of the electrode is 120 µm. Roasted seaweed (Nagai NoRi Co., Ltd; Torrance, CA), a popular snack and also heavily used in sushi, was used as one of the possible separators. Seaweed consists of multilayer hydrophilic structures with high electrical resistivity and high ion permeability. Finally, the supercapacitor was assembled by laminating roasted seaweed (Nagai NoRi Co., Ltd; Torrance, CA) as separator between two electrodes and thermal sealing of gelatin sheets as package (Modernist Pantry, LLC; York, ME). Between the gelatin sheets and collectors, cheese slices were placed to avoid the absorption of electrolyte by gelatin.

The specific capacitance ($C_{sp}$) was calculated from the slope of the discharge capacitance $C_{sp} = \frac{2I}{m\left(\frac{\Delta V}{\Delta t}\right)}$, where $I$ is the applied current and $m$ is the average mass of the two electrodes. EIS studies were performed by applying a small perturbation voltage of 5 mV in the frequency range of 0.01 Hz to 100 kHz. The energy and power density were calculated by conducting galvanostatic charge–discharge cycling with constant current densities ranging from 250 mA $g^{-1}$ to 4 A $g^{-1}$.

*Antimicrobial Susceptibility Testing with Edible Supercapacitor*: The electrode dimension used in the supercapacitor-bacterial susceptibility experiments was 2 cm × 4 cm. The seaweed separator was first soaked with Gatorade electrolyte and then laminated between two electrodes. Subsequently, the entire sandwiched structure was curled into a roll and inserted into a standard 000 size gelatin capsule body (diameter 9.55 mm). The two current collector tabs were pulled out through the two openings on the capsule cap. Finally, both openings were sealed by edible birthday candle wax (LolliZ Co.; Poway, CA).

Exponential phase cultures of *E. coli* ATCC 25922 were prepared by diluting overnight cultures into cation-adjusted Mueller Hinton broth, followed by growth to an $OD_{600}$ of ≈0.09 (≈$10^7$ CFU $mL^{-1}$) at 37 °C with gentle rotary mixing in Cation-Adjusted Mueller-Hinton Broth (CAMHB), which is nutrient dense and allows the bacteria to grow exponentially. The media were then switched to PBS solution, which allows for survival of the *E. coli* but futher reproduction will be suppressed. The cells were twice pelleted by centrifugation and resuspended in PBS. The cells were transferred to a 40 mL cylindrical glass tube, and current was introduced to the medium via the supercapacitor. A growth control, without supercapacitor-driven electric current, was used to establish bacterial viability in PBS.

Two brass rods, held secure with a rubber stopper, were inserted into the 3 mL *E. coli* suspension in a vial. The electric current loop was formed by connecting the outside ends of the rods with the supercapacitor. A current release cycle consisted of a current pulse stage by connecting with supercapacitor for 2 min followed with a rest stage by disconnecting the supercapacitor for another 2 min. All experiments

were performed in a 37 °C warm room. Bacterial samples were collected every 15 min for 60 min. Bacterial cell survival was determined by plating duplicate tenfold serial dilutions for each sample on Mueller Hinton agar and enumerating colonies on plates following overnight incubation at 37 °C.

For all other methods and details, refer to the Supporting Information.

## Supporting Information

Supporting Information is available from the Wiley Online Library or from the author.

## Acknowledgements

X.W., W.X., and P.C. contributed equally to this work. The authors acknowledge the financial support from the Office of Associate Dean for Research at Ira A. Fulton School of Engineering, and Office of Knowledge Enterprise and Development, Arizona State University. H.J. acknowledges the support from NSF CMMI-1067947 and CMMI-1162619.

Received: April 4, 2016
Revised: April 18, 2016
Published online:

[1] G. Deuschl, C. Schade-Brittinger, P. Krack, J. Volkmann, H. Schäfer, K. Bötzel, C. Daniels, A. Deutschländer, U. Dillmann, W. Eisner, D. Gruber, W. Hamel, J. Herzog, R. Hilker, S. Klebe, M. Kloß, J. Koy, M. Krause, A. Kupsch, D. Lorenz, S. Lorenzl, H. M. Mehdorn, J. R. Moringlane, W. Oertel, M. O. Pinsker, H. Reichmann, A. Reuß, G. H. Schneider, A. Schnitzler, U. Steude, V. Sturm, L. Timmermann, V. Tronnier, T. Trottenberg, L. Wojtecki, E. Wolf, W. Poewe, J. Voges, *N. Engl. J. Med.* **2006**, *355*, 896.

[2] E. Ben-Menachem, R. Mañon-Espaillat, R. Ristanovic, B. J. Wilder, H. Stefan, W. Mirza, W. B. Tarver, J. F. Wernicke, *Epilepsia* **1994**, *35*, 616.

[3] A. T. Assaf, S. Hillerup, J. Rostgaard, M. Puche, M. Blessmann, C. Kohlmeier, P. Pohlenz, J. C. Klatt, M. Heiland, A. Caparso, F. Papay, *Int. J. Oral Maxillofac. Surg.* **2015**, *45*, 245.

[4] W. V. Tamborlane, R. S. Sherwin, M. Genel, P. Felig, *N. Engl. J. Med.* **1979**, *300*, 573.

[5] J. Pickup, H. Keen, *Diabetes Care* **2002**, *25*, 593.

[6] S. W. Hwang, H Tao, D. H. Kim, H. Cheng, J. K. Song, E. Rill, M. A. Brenckle, B. Panilaitis, S. M. Won, Y. S. Kim, Y. M. Song, K. J. Yu, A. Ameen, R. Li, Y. Su, M. Yang, D. L. Kaplan, M. R. Zakin, M. J. Slepian, Y. Huang, F. G. Omenetto, J. A. Rogers, *Science* **2012**, *337*, 1640.

[7] X. Huang, Y. Liu, S. W. Hwang, S. K. Kang, D. Patnaik, J. F. Cortes, J. A. Rogers, *Adv. Mater.* **2014**, *26*, 7371.

[8] S. W. Hwang, J. K. Song, X. Huang, H. Cheng, S. K. Kang, B. H. Kim, J. H. Kim, S. Yu, Y. Huang, J. A. Rogers, *Adv. Mater.* **2014**, *26*, 3905.

[9] L. Yin, X. Huang, H. Xu, Y. Zhang, J. Lam, J. Cheng, J. A. Rogers, *Adv. Mater.* **2014**, *26*, 3879.

[10] S. W. Hwang, C. H. Lee, H. Cheng, J. W. Jeong, S. K. Kang, J. H. Kim, J. Shin, J. Yang, Z. Liu, G. A. Ameer, Y. Huang, J. A. Rogers, *Nano Lett.* **2015**, *15*, 2801.

[11] S. K. Kang, S. W. Hwang, S. Yu, J. H. Seo, E. A. Corbin, J. Shin, D. S. Wie, R. Bashir, Z. Ma, J. A. Rogers, *Adv. Funct. Mater.* **2015**, *25*, 1789.

[12] M. Irimia-Vladu, P. A. Troshin, M. Reisinger, L. Shmygleva, Y. Kanbur, G. Schwabegger, M. Bodea, R. Schwödiauer, A. Mumyatov, J. W. Fergus, V. F. Razumov, H. Sitter, N. S. Sariciftci, S. Bauer, *Adv. Funct. Mater.* **2010**, *20*, 4069.

[13] M. Irimia-Vladu, E. D. Głowacki, P. A. Troshin, G. Schwabegger, L. Leonat, D. K. Susarova, O. Krystal, M. Ullah, Y. Kanbur, M. A. Bodea, V. F. Razumov, H. Sitter, S. Bauer, N. S. Sariciftci, *Adv. Mater.* **2012**, *24*, 375.

[14] M. Irimia-Vladu, E. D. Głowacki, G. Voss, S. Bauer, N. S. Sariciftci, *Mater. Today* **2012**, *15*, 340.

[15] C. J. Bettinger, Z. Bao, *Adv. Mater.* **2010**, *22*, 651.

[16] H. Tao, D. L. Kaplan, F. G. Omenetto, *Adv. Mater.* **2012**, *24*, 2824.

[17] M. Irimia-Vladu, *Chem. Soc. Rev.* **2014**, *43*, 588.

[18] C. J. Bettinger, *Trends Biotechnol.* **2015**, *33*, 575.

[19] Y. J. Kim, S. E. Chun, J. Whitacre, C. J. Bettinger, *J. Mater. Chem. B* **2013**, *1*, 3781.

[20] Y. J. Kim, W. Wu, S. E. Chun, J. F. Whitacre, C. J. Bettinger, *Proc. Natl. Acad. Sci. U.S.A.* **2013**, *110*, 20912.

[21] Z. Li, D. Young, K. Xiang, W. C. Carter, Y. M. Chiang, *Adv. Energy Mater.* **2013**, *3*, 290.

[22] W. Wu, A. Mohamed, J. F. Whitacre, *J. Electrochem. Soc.* **2013**, *163*, A497.

[23] J. Yan, Q. Wang, T. Wei, Z. Fan, *Adv. Energy Mater.* **2014**, *4*, 4.

[24] D. G. Siegel, K. E. Church, G. R. Schmidt, *J. Food Sci.* **1979**, *44*, 1276.

[25] A. Gennadios, A. Handa, G. W. Froning, C. L. Weller, M. A. Hanna, *J. Agric. Food Chem.* **1998**, *46*, 1297.

[26] G. H. Lu, T. C. Chen. *J. Food Eng.* **1999**, *42*, 147.

[27] P. J. Neuvonen, *Clin. Pharmacokinet.* **1982**, *7*, 465.

[28] P. J. Neuvonen, K. T. Olkkola, *Med. Toxicol. Adverse Drug Exper.* **1988**, *3*, 33.

[29] C. L. Dorrington, D. W. Johnson, R. Brant, *Ann. Emergency Med.* **2003**, *41*, 370.

[30] M. M. Welz, C. M. Ofner, *J. Pharm. Sci.* **1992**, *81*, 85.

[31] G. A. Digenis, T. B. Gold, V. P. Shah, *J. Pharm. Sci.* **1994**, *83*, 915.

[32] C. M. Ofner, Y. E. Zhang, V. C. Jobeck, B. J. Bowman, *J. Pharm. Sci.* **2001**, *90*, 79.

[33] L. L. Zhang, X. S. Zhao, *Chem. Soc. Rev.* **2009**, *38*, 2520.

[34] S. D. Barranco, J. A. Spadaro, T. J. Berger, R. O. Becker, *Clin. Orthop. Relat. Res.* **1974**, *100*, 250.

[35] C. P. Davis, N. Wagle, M. D. Anderson, M. M. Warren, *Antimicrob. Agents Chemother.* **1991**, *35*, 2131.

[36] T. Matsunaga, S. Nakasono, S. Masuda, *FEMS Microbiol. Lett.* **1992**, *72*, 255.

[37] T. Matsunaga, S. Nakasono, T. Takamuku, J. G. Burgess, N. Nakamura, K. Sode, *Appl. Environ. Microbiol.* **1992**, *58*, 686.

[38] Z. Król, A. Jarmoluk, *J. Food Eng.* **2016**, *170*, 1.

[39] J. L. d. Pozo, M. S. Rouse, J. N. Mandrekar, J. M. Steckelberg, R. Patel, *Antimicrobial. Agents Chemother.* **2009**, *53*, 41.

[40] E. L. Sandvik, B. R. McLeod, A. E. Parker, P. S. Stewart, *PloS One* **2013**, *8*, e55118.

ADVANCED MATERIALS TECHNOLOGIES

# Supporting Information

for *Adv. Mater. Technol.*, DOI: 10.1002/admt.201600059

## Food-Materials-Based Edible Supercapacitors

*Xu Wang, Wenwen Xu, Prithwish Chatterjee, Cheng Lv, John Popovich, Zeming Song, Lenore Dai, M. Yashar S. Kalani, Shelley E. Haydel, and Hanqing Jiang**

WILEY-VCH

# Supplementary Information

## Food Materials Based Edible Supercapacitors

*Xu Wang#, Wenwen Xu#, Prithwish Chatterjee#, Cheng Lv, John Popovich, Zeming Song, Lenore Dai, M. Yashar S. Kalani, Shelley E. Haydel,* and *Hanqing Jiang**

*#These authors contribute equally.*

[*] Prof. Hanqing Jiang
School for Engineering of Matter, Transport and Energy, *Arizona State University, Tempe, AZ 85287, USA*
*Email:* hanqing.jiang@asu.edu
Xu Wang, Wenwen Xu, Dr. Prithwish Chatterjee, Cheng Lv, Zeming Song and Prof. Lenore Dai
School for Engineering of Matter, Transport and Energy, *Arizona State University, Tempe, AZ 85287, USA*
John Popovich *and Prof.* Shelley E. Haydel
School of Life Sciences, *Arizona State University, Tempe, AZ 85287, USA*
Dr. M. Yashar S. Kalani
Division of Neurological Surgery, Barrow Neurological Institute, St. Joseph's Hospital and Medical Centre, Phoenix, AZ 85003, USA
*Prof.* Shelley E. Haydel
Center for Infectious Diseases and Vaccinology, The Biodesign Institute, *Arizona State University, Tempe, AZ 85287, USA*

*Keywords:* edible materials, food, supercapacitors, anti-bacteria, power source.

*Brunauer–Emmett–Teller (BET) test*: The activated charcoal used as the supercapacitor electrodes was initially dried at 150°C to remove any moisture from the surface. The adsorption analysis was carried out with a Micromeritics ASAP2000. Specifically, 0.1 grams of the activated charcoal was loaded in the tube with nitrogen flowing at 2 bar pressure for 4 hours. Adsorption was analyzed using the BET module. The results revealed a surface area of ~1,400 $m^2$ $g^{-1}$ for the activated charcoal (Fig. 1d).

*Permittivity test*: The seaweed and rice paper were studied for their permittivity using deionized water as the passing fluid. Briefly, 2-inch diameter sections of seaweed and rice paper were cut out using a circular stamp. The testing material (i.e., seaweed and rice paper) was placed at the end of a 5-inch steel chamber using a rubber gasket. Water was poured into the chamber, and the sequential pressure test was performed using regulated nitrogen from a cylinder. The fluid passing out from the chamber was collected in a beaker and placed on a weighing balance, which was connected to a computer. The data from the fluid pass was used to calculate mass flux and permittivity.

*In-situ 2D observation of gelatin sheet digestion in simulated gastric fluid*: A gelatin sheet with dimensions of 160 µm (thickness) × 1,090 µm × 4,000 µm was used for the observation. Fig. S1 presents the experiment setup. The gelatin sheet was held vertically by a sponge stage in a glass dish under an optical microscope in room temperature 25 $C^o$. The sponge stage was able to keep the gelatin sheet standing in the glass dish and impose mechanical constraints in the horizontal direction. For the thin gelatin film that swells isotropically, the force required to constrain the deformation in the horizontal direction is

much smaller than that in the thickness direction. Under the same swelling strain, small cross-sectional area in the thickness direction exerts much less force in the horizontal direction compared that in the thickness direction. To implement this in experiments, by surrounding the gelatin film with sponge, the sponge is able to confine the gelatin film horizontally, while leave the films relatively free to swell in the thickness direction. The simulated gastric fluid was composed of 2.0 g of sodium chloride and 3.2 g of purified pepsin (derived from porcine stomach mucosa, with an activity of 800 to 2,500 units per mg of protein) in 7.0 mL of hydrochloric acid (HCl) and water (1000 mL). This test solution has a pH of about 1.2. When the sponge was soaked with simulated gastric fluid and touched the gelatin sheet, it could be used to simulate the gelatin sheet in stomach environment. After the simulated gastric fluid was poured into the glass dish, swelling and digestion of the gelatin sheet were observed *in-situ* by microscopy (Nikon eclipse lv100). It was observed that a gelatin sheet with an initial cross-sectional area of 160 μm × 1,090 μm first swells due to the diffusion of the gastric fluid into the polymeric gelatin network, and then shrinks due to the digestion of gelatin and eventually becomes undetectable microscopically (Nikon eclipse lv100, 5X objective) after 2.5 hours. During this process (swelling → shrinking), because of the constraint in the horizontal direction, the maximum strain in the horizontal direction $\varepsilon_{horizontal}$ was only 17%, while its counterpart in the thickness direction $\varepsilon_{thickness}$ was 261%. This quasi-one-dimensional constrained digestion process can be understood by a theoretical model that considers the coupling of mass diffusion, chemical reaction, and extremely large mechanical deformation.

*Modelling of gelatin sheet digestion and implementation of a 1D case*: A theoretical model was developed to characterize the digestive process. This model considers the coupling of mass diffusion, chemical reaction, as well as the nonlinear mechanical behavior. The mixture of gelatin and HCl forms a gel, with the former as polymeric network and later as solvent.

The general time-dependent diffusion equation with Fickian first law is used to model the diffusion of HCl in gelatin, i.e.

$$\frac{d}{dt}\int_V C dV + \int_a j_i n_i da = r\,, \tag{1}$$

$$j_i = cD\frac{\partial \bar{\mu}}{\partial x_i}, \tag{2}$$

where $C$ and $c$ are the nominal and true concentration of HCl in gel; $V$ is the initial volume of gel; $\mathbf{j}$ is true flux of HCl into the gel; $a$ is current area of gel; $\mathbf{n}$ is the normal vector of a surface in the current state; $r$ is the source of HCl generation; $D$ [unit: $m^2\ s^{-1}$] is the diffusivity of HCL into the gelatin network; $\bar{\mu} = \mu / RT$ is the normalized chemical potential of HCL with $R$ gas constant and $T$ temperature; $x_i$ are the coordinates of the current state where the subscript $i$ varies from 1 to 3.

The first-order chemical reaction model is applied here as the source of HCl generation, i.e.

$$r = \int_V kC dV \tag{3}$$

where $k$ is the first-order reaction constant [1].

For nonlinear material behavior of the gelatin, the normalized free energy can be written as [2, 3],

$$\bar{W}\left(\mathbf{F}^{diff},C\right)=\frac{W\left(\mathbf{F}^{diff},C\right)}{RT/v}=\frac{W_s\left(\mathbf{F}^{diff}\right)+W_m\left(C\right)}{RT/v}$$
$$=\frac{1}{2}nv\left[F_{iK}^{diff}F_{iK}^{diff}-3-2\ln\left(\det\mathbf{F}^{diff}\right)\right]+RT\left[C\ln\left(\frac{Cv}{1+BC}\right)+\frac{\chi C}{1+BC}\right] \quad (4)$$

Here, the deformation gradient $\mathbf{F}=\partial\mathbf{x}/\partial\mathbf{X}$ is decomposed into the mechanical stretch part and chemical reaction part using polar decomposition, i.e., $\mathbf{F}=\mathbf{F}^{diff}\cdot\mathbf{F}^{rec}$, where $\mathbf{F}^{diff}$ is the diffusion induced deformation and $\mathbf{F}^{rec}$ represents the chemical reaction induced deformation. $\mathbf{F}^{diff}$ stretches the polymeric network, and $\mathbf{F}^{rec}$ eliminates materials (i.e., digestion) (i.e., $\det\left(\mathbf{F}^{rec}\right)<1$). $W_s\left(\mathbf{F}^{diff}\right)$ and $W_m\left(C\right)$ are the stretch energy (depending on $\mathbf{F}^{diff}$) and mixing energy (depending on nominal concentration *C*), respectively. $\chi$ is the dimensionless parameter that relates to the enthalpy of mixing. $n$ is the molar number of chain divided by the dry volume of gel with a unit of $mol/m^3$, $v$ is the molar volume of HCl.

The incompressibility assumption is applied, i.e., all particles (solvent and polymers) are incompressible, which leads to

$$1+Cv-kCtn_AV_A=1+\left(v-ktn_AV_A\right)C=1+BC=\det\mathbf{F}, \quad (5)$$

and

$$1+Cv=\det\mathbf{F}^{diff} \quad (6)$$

where $V_A$ is the molar volume of gelatin; $n_A$ is the molar ratio between the reactant (gelatin) and the solvent (HCl) in the chemical reaction balance, and $t$ is the time.

Substitute Eq. (5) into Eq. (4) and use the Legendre transformation, a modified normalized free energy is given by

$$\hat{W}\left(\mathbf{F}^{diff},\mathbf{F},\mu\right)=\bar{W}-\mu C, \quad (7)$$

Where $\hat{W}$ is defined as a function of $\mathbf{F}^{diff}$, $\mathbf{F}$ and $\mu$.

Due to chemical reaction, the reduction of the material affects the reference volume, which leads the free energy by considering the chemical reactions

$$\hat{W}\left(\mathbf{F}^{diff},\mathbf{F},\mu\right)V' = \tilde{W}\left(\mathbf{F}^{diff},\mathbf{F},\mu\right)V\ . \tag{8}$$

Here $V' = V\det\mathbf{F}^{rec}$ is the reduced volume of gel considering the effect of chemical reaction and $\tilde{W}\left(\mathbf{F}^{diff},\mathbf{F},\mu\right)$ is the modified free energy. Thus, the nominal stress is given by

$$\mathbf{s} = \frac{RT}{v}\frac{\partial\tilde{W}\left(\mathbf{F}^{diff},\mathbf{F},\mu\right)}{\partial\mathbf{F}^{diff}} \tag{9}$$

As shown in Fig. 1h, the change of the horizontal stretch ratio $\lambda_{horizontal}$ was much smaller compared with that in the thickness direction $\lambda_{thickness}$. Therefore, a 1D model can be applied based on the general 3D model. Thus the deformation gradient can be written as:

$$\mathbf{F} = \mathbf{F}_c\mathbf{F}_r = \begin{pmatrix}1&0&0\\0&1&0\\0&0&\lambda_3\end{pmatrix} = \begin{pmatrix}1&0&0\\0&1&0\\0&0&\lambda_{3c}\end{pmatrix}\begin{pmatrix}1&0&0\\0&1&0\\0&0&\lambda_{3r}\end{pmatrix} \tag{10}$$

where the horizontal stretch ratios due to diffusion and chemical reaction are fixed to be one. $\lambda_3 = \lambda_{thickness}$ will be the only value to be calculated in the following analysis, and $\lambda_3 = \lambda_{3c}\lambda_{3r}$ with $\lambda_{3c}$ the stretch ratio for diffusion and $\lambda_{3r}$ for chemical reaction.

Combining Eq. (1) to (10), the time-dependent partial differential equation (PDE) of $\lambda_3$ can be obtained as:

$$\frac{1}{\lambda_1^2\lambda_3}\lambda_1^2\frac{\partial\lambda_3}{\partial t}=\frac{\partial}{\partial x_3}\left[\frac{D\left(\lambda_1^2\lambda_3-1\right)}{\lambda_1^2\lambda_3}\frac{\partial\overline{\mu}}{\partial x_3}\right]-\frac{k\left(\lambda_1^2\lambda_3-1\right)}{\lambda_1^2\lambda_3}\left(1+\frac{n_A V_A}{B}\right) \tag{11}$$

where

$$\overline{\mu}\left(X_3,t\right)=\frac{\begin{array}{c}3\frac{\partial\lambda_{3r}}{\partial\lambda_3}\left\{\frac{1}{2}nB\left[2\lambda_1^2+\frac{\lambda_3^2}{\lambda_{3r}^2}-3-2\ln\left(\frac{\lambda_1^2\lambda_3}{\lambda_{3r}}\right)\right]+\left(\lambda_1^2\lambda_3-1\right)\ln\left(\frac{\lambda_1^2\lambda_3-1}{B\lambda_1^2\lambda_3}v\right)+\frac{\lambda_1^2\lambda_3-1}{\lambda_1^2\lambda_3}\chi_1\right\}\\+\lambda_{3r}\left\{nB\left[\frac{v}{B\lambda_1^2}+\frac{v^2\lambda_3}{B^2}-\frac{v^2}{B^2\lambda_1^2}-\frac{\lambda_1^2 v}{B+\left(\lambda_1^2\lambda_3-1\right)v}\right]+\frac{1}{\lambda_3}+\lambda_1^2\ln\left(\frac{\left(\lambda_1^2\lambda_3-1\right)v}{B\lambda_1^2\lambda_3}\right)+\frac{\chi_1}{\lambda_1^2\lambda_3^2}\right\}\end{array}}{3\left(\lambda_1^2\lambda_3-1\right)\frac{\partial\lambda_{3r}}{\partial\lambda_3}+\lambda_1^2\lambda_{3r}},$$

The PDE shown above was solved by using commercial software COMSOL, specifically using the coefficient form PDE module. The following material properties were used. Shear modulus $nRT=33.3kPa$ and the value of $RT/v=4\times10^7 Pa$, $v=1\times10^{-5}m^3/mol$ were adopted from references [2, 4, 5]. Using the free swelling ratio of the gelatin without chemical reaction, $\chi_1=0.554$ was determined. Two fitting parameters were used. One is the diffusivity $D=8\times10^{-10}m^2/s$, which was obtained through fitting the short-time limit of the stretch ratio $\lambda_{thickness}$ from experiment. Another is the first-order reaction constant $k=8\times10^{-5}/s$, which was obtained by fitting the long-time limit of the stretch ratio $\lambda_{thickness}$ from experiment. Vanishing flux (i.e. $\frac{\partial\overline{\mu}}{\partial x_3}=0$) and chemical potential (i.e., $\overline{\mu}=0$) boundary conditions were applied at two ends of this 1D problem.

*Other food materials for edible supercapacitor*: Table S1 shows materials (food) that have been studied as components of the edible supercapacitors. For columns,

(1) Binders: In addition to egg white, CMC, a cellulose derivative with

carboxymethyl groups bound to the hydroxyl groups of the glucopyranose monomers that make up the cellulose backbone, has also been applied as binder. CMC is widely used in the food industry as a viscosity modifier, thickener, or stabilizer to stabilize emulsions and serve as a binder.

(2) Current collectors: In addition to gold leaves, silver leaves were also used. Both gold and silver leaves are used for decorating cakes.

(3) Electrolytes: Besides Gatorade sports drink, lemon juice, Monster energy drink, and V8 vegetable juice have been studied as possible electrolytes. All of these drinks contain large amounts of transportable free sodium or potassium ions and anions. Moreover, a surprising discovery is that the homemade jello, cheese, and BBQ sauce work efficiently as electrolytes. For jello and cheese, separators are not needed, since these food products are efficient electrolytes. In order to increase the ionic concentration, monosodium glutamate (MSG) has been added as an electrolyte additive. MSG is the sodium salt of glutamic acid, commonly used in the food industry as a flavor enhancer.

(4) Separators: In addition to seaweed, rice paper was also studied as a separator. Both seaweed and rice paper have the ability to maintain electrolytes and allow the transportation of ions.

(5) Segregation layer: For all liquid electrolytes, we used cheese as segregation layers. For solid electrolytes, the segregation layer is not needed.

(6) Packaging materials: We have studied gelatin and gummy candy as packaging materials.

*Edible supercapacitor lighting up light-emitting diodes (LED)*: The supercapacitor set consists of three supercapacitors connected in series. The electrode area is 2 cm × 2 cm with an average mass loading of 0.02 g. For LED lighting inside simulated gastric fluid, two-thirds of the supercapacitor body was immersed in the fluid. The LED stayed on for three minutes, followed by gradual dimming and lack of emission after four minutes. After one hour, the supercapacitor was partially dissolved in the simulated gastric fluid. For LED lighting outside simulated gastric fluid, two-thirds of the supercapacitor body was immersed in the fluid. The LED stayed on for 10 minutes.

*Wireless charging system*: The wireless charging system consists of a transmitter chamber, in which supercapacitors will be placed, and a receiver lid, with which supercapacitors will be connected. The transmitter chamber was fabricated by winding 17 turns of copper wire on the outside wall of a glass tube (diameter 72.2 cm, height 40.1 cm). A transmitter circuit (GHH, Amazon) was then connected with coil and taped on the wall. The main function of the transmitter circuit is to convert direct current to alternating current with a frequency of 60 Hz. Thus, an alternating electromagnetic field will be created in this chamber by the alternating current. The receiver lid was fabricated by winding 19 turns of copper wire on the surface of a lid made of rice paper and copy paper. 2 more turns was used in the receiver end to increase the reliability of the system and to ensure that the 5V signal to transmitter end will be fully received. A receiver from the same transmitter-receiver module (GHH, Amazon) was then mounted at the center of the lid and connected with the receiver coil. The supercapacitor can be connected with the receiver lid through the two openings on the lid.

*Edible supercapacitor charged in wireless charging system*: Five supercapacitors (electrode area 4 cm × 4 cm) connected in series were placed in the charging chamber and initially connected with the receiver lid of the wireless charging system (Fig. S6a). Before charging, the supercapacitors were discharged to less than 0.5 V (Fig. S6b). The supercapacitor set was not able to light up the LED after the initial discharge. The supercapacitor set was then charged by connecting a 5V constant voltage source to the transmitter of the wireless charging system on the outside wall of the charging chamber. It was also connected with a voltage meter to monitor and record voltage changes during charging. After 5 minutes of constant voltage charge, the supercapacitor set reached 5V (Fig. S6c) and was able to light up the LED (Fig. S6d). The supercapacitor was then disconnected from the receiver of the wireless charging system and removed from the charging chamber (Fig. S6e). The removed edible supercapacitor set was shown to light up the LED (Fig. S6f).

**Supplementary Figures**

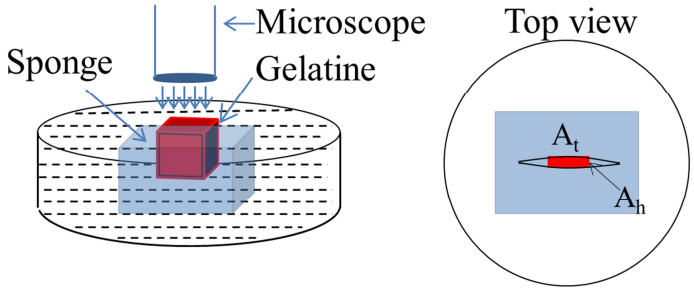


**Supplementary Figure S1. Gelatin sheet digestion experiment setup.** The gelatin was held vertically by a sponge stage in a glass dish filled with simulated gastric fluid under an optical microscope. The porous sponge was able to keep the gelatin sheet standing in the glass dish and imposed mechanical constraints in the horizontal direction.

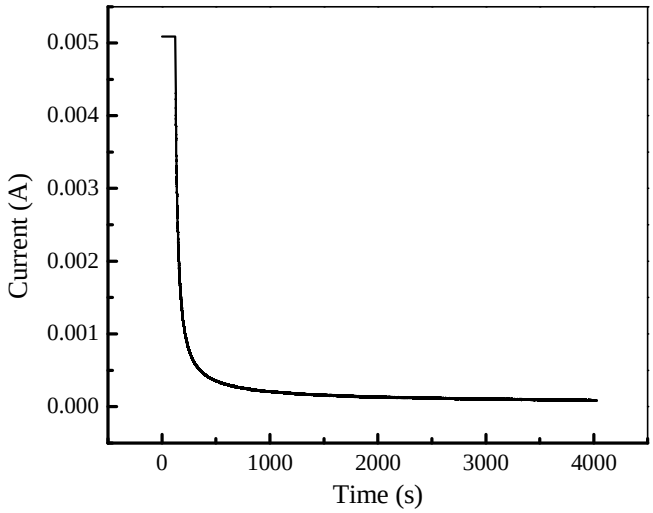


**Supplementary Figure S2. Leakage current measurement.** After a 5mA constant current charging to 1V and 1V constant voltage charging for 1 hour, the current drop to 0.08mA, which is determined to be the leakage current.

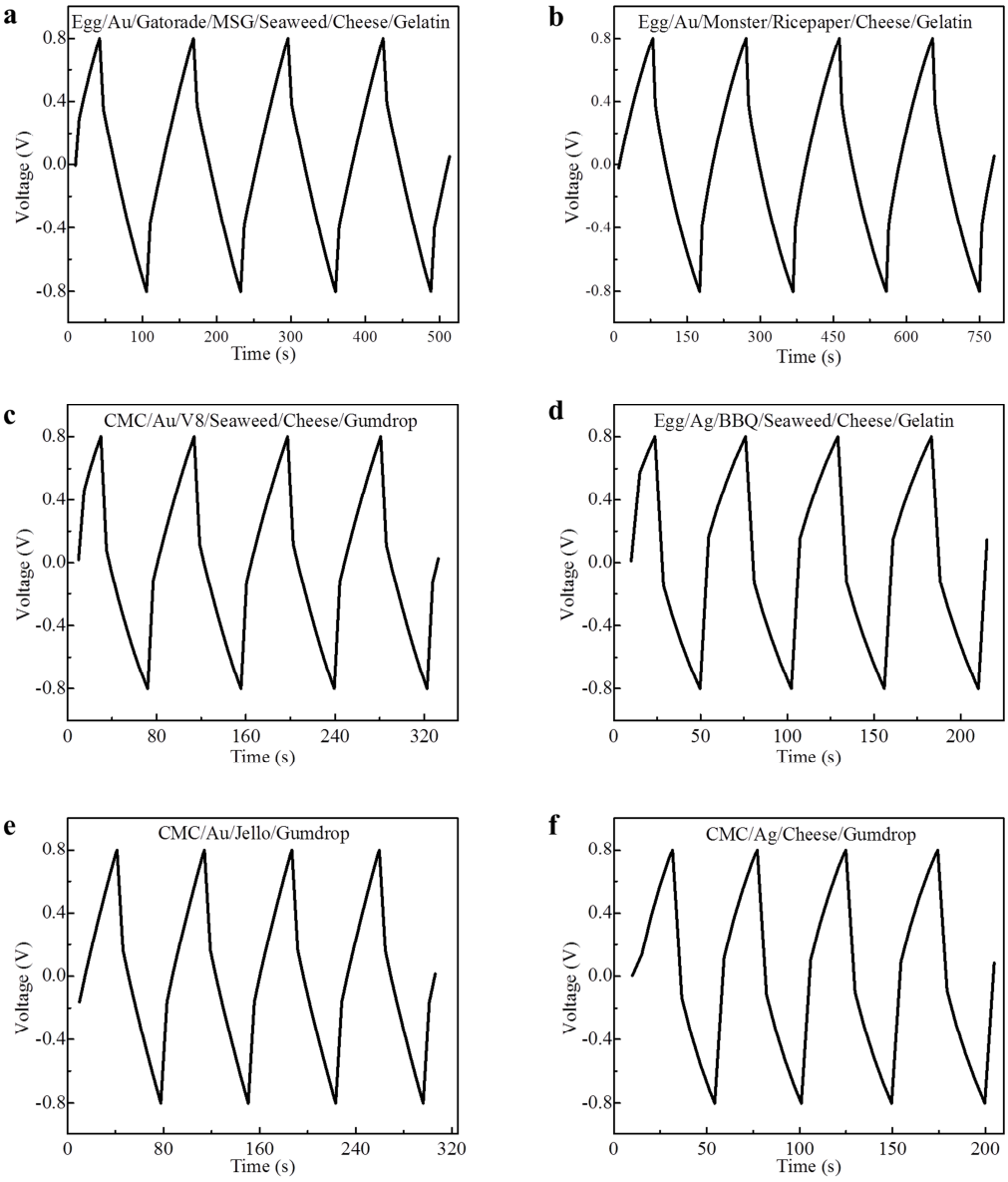


**Supplementary Figure S3. Galvanostatic charge-discharge curves for different material combinations at the current density of 1 A $g^{-1}$.** The galvanostatic charge-discharge curves for different material combinations at the current density of 1 A $g^{-1}$ are shown. For supercapacitors with Gatorade sports drink (**a**) or Monster energy drink (**b**)

serving as the liquid electrolyte, the internal resistance drop is small compared to those with the V8 vegetable juice (**c**) or jello (**e**) electrolyte.

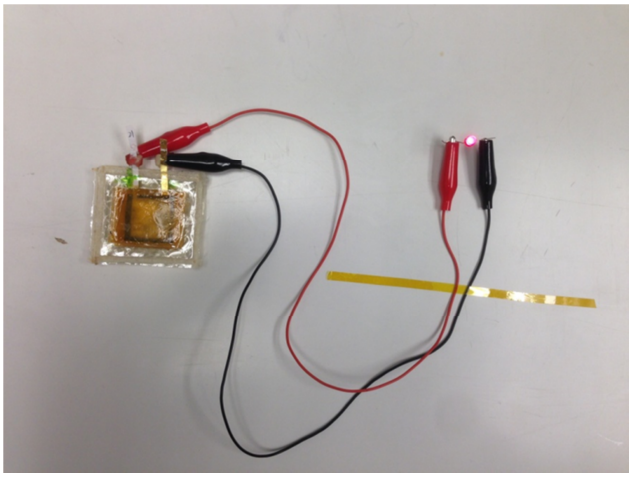

**Supplementary Figure S4. Edible supercapacitor lighting up the LED outside of gastric fluid.** The LED stays lit for about 10 minutes.

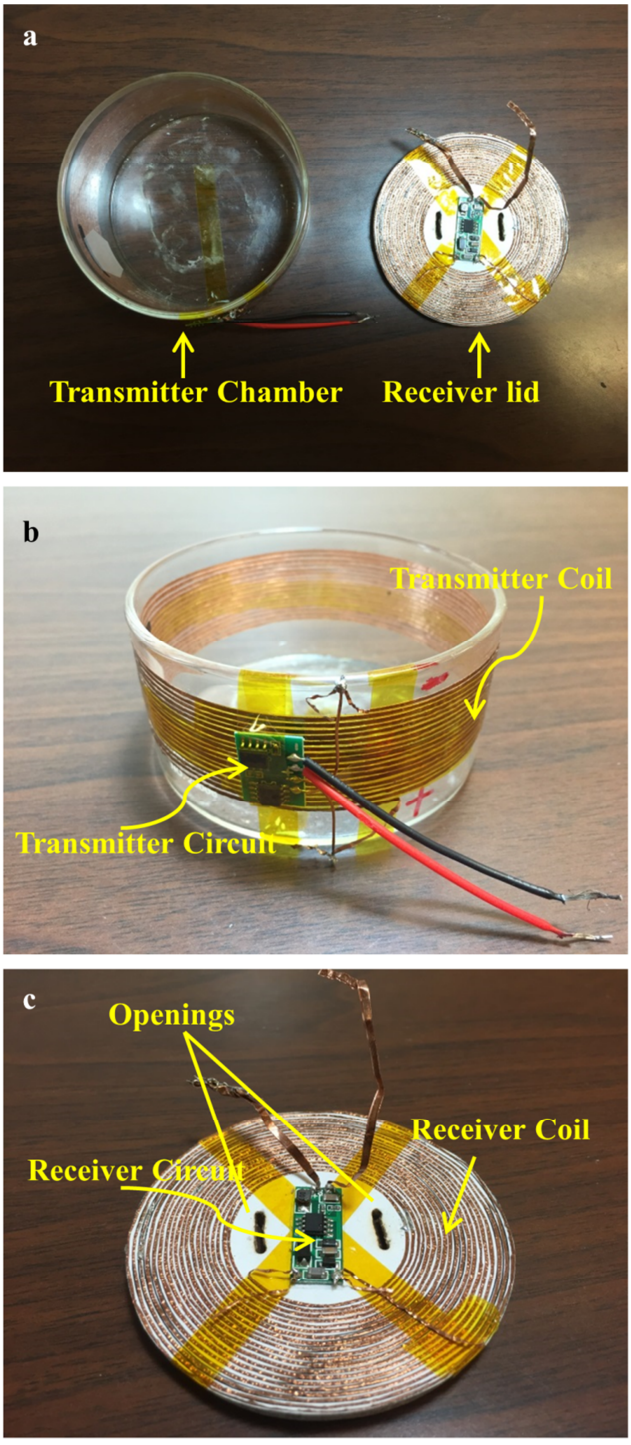


**Supplementary Figure S5. Wireless charging system.** (**a**) Top view of wireless charging system, consisting of a transmitter chamber and a receiver lid. (**b**) Transmitter chamber consists of transmitter coil and circuit on the outside wall of a glass tube. (**c**)

Receiver lid consists of receiver circuit and receiver coil on the surface of a circular lid made of rice paper and copy paper.

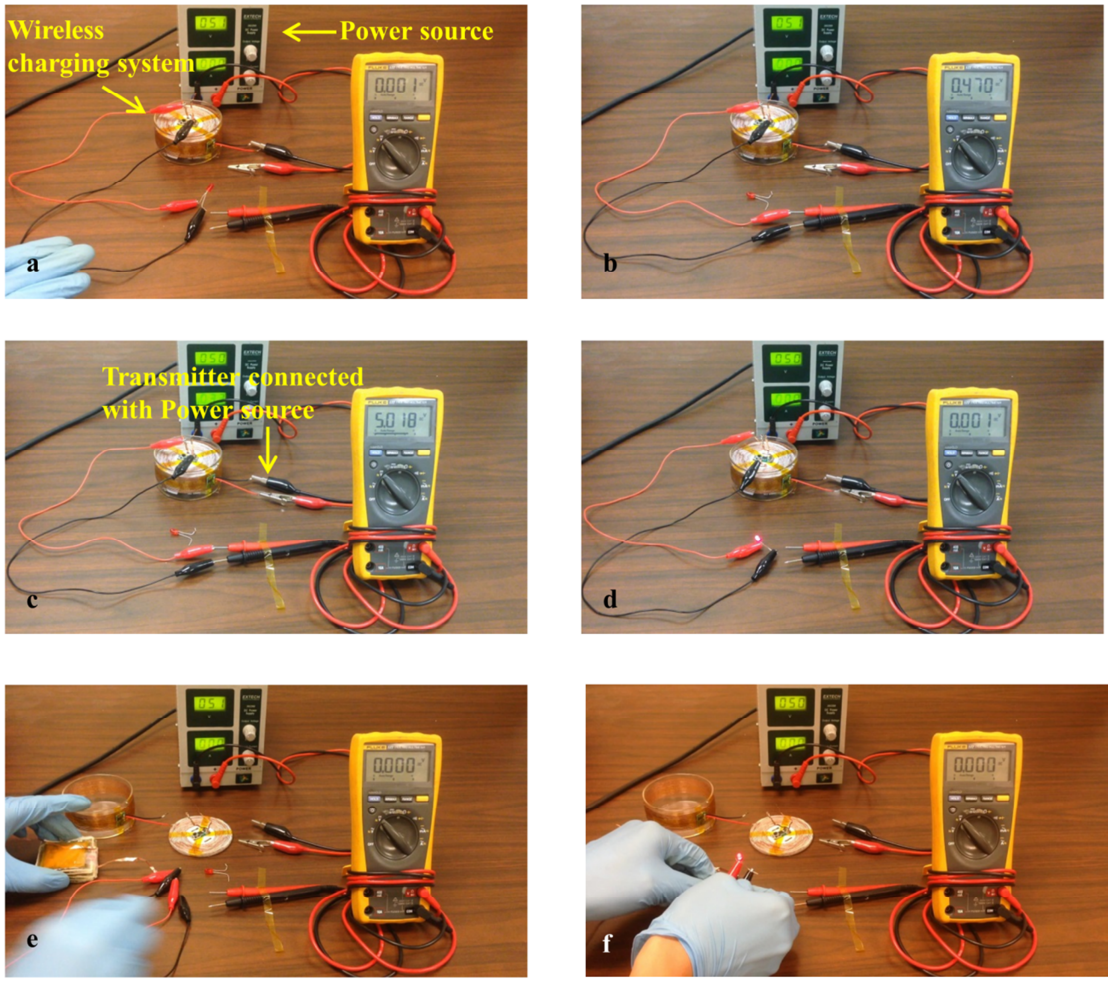


**Supplementary Figure S6. Edible supercapacitor charged in a wireless charging system.** (**a**) The setup consists of a constant voltage power source, wireless charging system, LED, and voltage meter. (**b**) The initial voltage of the supercapacitor set is 0.470 V. (**c**) The voltage of the supercapacitor set increases to 5.018V. (**d**) The supercapacitor set lights up a LED inside the charging chamber while the external power source is still wirelessly charging the supercapacitor. (**e**) The supercapacitor set is removed. (**f**) The supercapacitor set lights up a LED outside of the charging chamber.

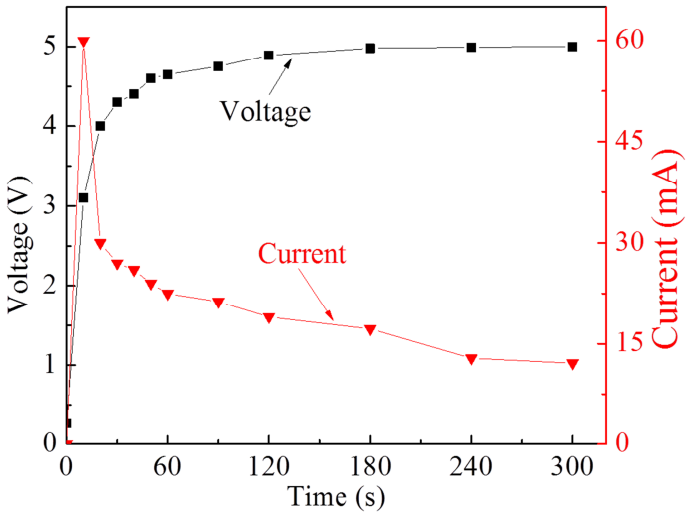


**Supplementary Figure S7. Edible supercapacitor current and voltage profiles during wireless charging.** With 5.144 V constant voltage output from the receiver, the voltage of the supercapacitor set increases from 0.470 to 4.994 V, and the current decreases from 60 (measured at 10s) to 14.41 mA in 3 minutes. After five minutes, the voltage increases to 5.002 V while the current drops to 12 mA.

**Supplementary Table S1. Food materials for edible supercapacitors**

| Binder | Current Collector | Electrolyte | Separator | Segregation layer | Package |
|---|---|---|---|---|---|
| **Egg** | Au | Gatorade+MSG | Seaweed | Cheese | Gelatin |
| **Egg** | Au | Monster drink | Rice Paper | Cheese | Gelatin |
| **CMC** | Au | V8 drink | Seaweed | Cheese | Gummy candy |
| **Egg** | Ag | BBQ sauce | Seaweed | --- | Gelatin |
| **CMC** | Au | Jello | --- | --- | Gummy candy |
| **CMC** | Ag | Cheese | --- | --- | Gummy candy |

**Supplementary Movie S1. Edible supercapacitor charged in a wireless charging system.** Five supercapacitors (electrode area 4 cm × 4 cm) connected in series were placed in the charging chamber and initially connected with the receiver lid of the wireless charging system. Before charging, the supercapacitors were discharged to less than 0.5 V so that it was unable to light up the LED. The supercapacitor set was then charged by connecting a 5 V constant voltage source to the transmitter of the wireless charging system on the outside wall of the charging chamber. It was also connected with a voltage meter to monitor and record the voltage change during charging. After 5 minutes constant voltage charge, the supercapacitor set reached 5 V and was able to light up the LED. The supercapacitor was then disconnected from the receiver of the wireless charging system and removed from the charging chamber. The removed edible supercapacitor set subsequently lights up the LED.

**Supplementary Movie S2. Edible supercapacitor powering up a USB endoscope inspection snake tube camera and being eaten.** The positive and negative (ground) power cables of the USB snake camera were cut off and only the data cables were connected to a computer for data transmission. Five fully charged 4 cm × 4 cm (electrode area) square supercapacitors were connected in series to output a 5 V voltage in order to drive the USB camera that requires minimum 3.3 V working voltage. The negative terminal of the supercapacitors was connected to the negative (ground) of the snake camera at the beginning to maintain the same reference potential between the computer and supercapacitor. After the positive terminal of the supercapacitors was connected with the positive cable of the snake camera, the camera was recognized and

output a 320 × 240 pixels video on the computer screen. By sweeping the camera back and forth pointing at the computer screen, the image from the camera was captured and shown on the computer screen. The power cables were then disconnected with the supercapacitors and then one of the supercapacitors were removed and cut open. Finally, the removed supercapacitor was eaten and swallowed.

[1] S. W. Hwang, H Tao, D. H. Kim, H. Cheng, J. K. Song, E. Rill, M. A. Brenckle, B. Panilaitis, S. M. Won, Y. S. Kim, Y. M. Song, K. J. Yu, A. Ameen, R. Li, Y. Su, M. Yang, D. L. Kaplan, M. R. Zakin, M. J. Slepian, Y. Huang, F. G. Omenetto, J. A. Rogers, *Science* **2012,** 337, 1640.
[2] W. Hong, X. Zhao, J. Zhou, Z. Suo, *J. Mech. Phys. Solids* **2008**, 56, 1779.
[3] M. L. Huggins, *J. Chem. Phys.* **1941**, 9, 440.
[4] A. Karimi, M. Navidbakhsh, H. Yousefi, M. Alizadeh, *J. Thermoplast. Compos. Mater.* **2014**.
[5] J. L. Kavanagh, T. Menand, K. A. Daniels, *Tectonophysics* **2013**, 582, 101.